PERGAMON

International Journal of Heat and Mass Transfer 42 (1999) 127–142

International Journal of HEAT and MASS TRANSFER

# On the solution of inverse heat transfer problem using the Karhunen–Loève Galerkin method

H. M. Park*, O. Y. Chung, J. H. Lee

*Department of Chemical Engineering, Sogang University, Seoul, Korea*

Received 2 June 1997; in final form 27 March 1998

**Abstract**

An efficient method based on the Karhunen–Loève Galerkin procedure is proposed for the solution of inverse problem of estimating the time-varying strength of a heat source in a two-dimensional heat conduction system. The Karhunen–Loève Galerkin procedure converts a given system into a model with the minimum degree of freedom, and consequently the number of equations to be solved in the inverse analysis is minimized, resulting in the drastic reduction of computation time. The performance of the present technique of inverse analysis using the Karhunen–Loève Galerkin procedure is evaluated by several numerical experiments, and is found to be very accurate as well as efficient. 

**Nomenclature**

$a_i$ spectral coefficient premultiplying the $i$th empirical eigenfunction
$d(t)$ conjugate direction of the regular conjugate gradient method
$D(t)$ conjugate direction of the modified conjugate gradient method (equation 38)
$G(t)$ time-varying function of the dimensionless strength of heat source
$H_{ji}$ matrix defined in equation (11)
$J$ performance function defined in equation (14)
$K(x, x')$ two-point correlation function of the Karhunen–Loève decomposition
$ME$ number of basis functions employed in the Karhunen–Loève Galerkin procedure
$MO$ number of measuring points
$p_k(t)$ adjoint variable of the low dimensional model
$P(x, y, t)$ adjoint variable defined in equation (16)
$Q_{ijl}$ matrix defined in equation (12)
$R$ residual defined in equation (8)
$S_i$ vector defined in equation (13)
$t$ dimensionless time
$T$ dimensionless temperature field.

*Greek symbols*

$\alpha$ coefficient determining the dependence of thermal conductivity on temperature [cf. equation (6)]
$\gamma$ coefficient defined in equation (24)
$\delta$ Dirac delta function
$\delta a_i$ variation of the spectral coefficient $a_i$
$\delta J$ variation of the performance function
$\delta_n$ function defined by equation (5)
$\delta T$ variation of the dimensionless temperature field
$\kappa$ dimensionless thermal conductivity
$\lambda_k$ the $k$th eigenvalue [cf. equation (1)]
$\rho$ optimal step length in the conjugate gradient method
$\sigma$ standard deviation of measurement error
$\phi_i$ the $i$th empirical eigenfunctions
$\omega$ Gaussian distributed random number [cf. equation (52)]
$\Omega$ system domain
$\nabla J$ gradient of the performance function.

*Subscripts*

m measurement
mCG modified conjugate gradient method.

*Superscripts*

* experimental measurements
† position of heat source.

* Corresponding author.

0017–9310/98 $19.00 
PII: S0017–9310(98)00136–7

## 1. Introduction

Inverse heat transfer problems have numerous important applications in various branches of science and engineering. For example, the temperature of a very hot surface is not easily measured directly with sensors. Usually sensors are placed beneath the surface and the temperature of the hot surface is estimated by inverse analysis. Other examples of inverse heat transfer are the estimation of unknown space-dependent thermophysical properties of materials from the temperature recordings at the boundary surfaces of the domain.

Usually these inverse problems are ill-posed, i.e., the solution is not unique and sensitive to the measurement errors [1]. There are many methods now available which alleviate ill-poseness of inverse problems, e.g., the least square method modified by the addition of regularization term and the use of conjugate gradient method where the regularization is inherently built in the iterative procedure [2, 3].

In the present paper, we propose an efficient method based on the Karhunen–Loève Galerkin procedure for the solution of inverse heat transfer problem. The Karhunen–Loève decomposition is a technique enabling a stochastic field to be represented with a minimum degree of freedom. If the Karhunen–Loève decomposition is applied to a given stochastic field, we get a set of empirical eigenfunctions. When we want to reproduce that same stochastic field with a certain criterion of accuracy it can be represented with a minimum degree of freedom when employing these empirical eigenfunctions. A Galerkin method employing these empirical eigenfunctions of the Karhunen–Loève decomposition is called the Karhunen–Loève Galerkin method. Therefore, through the Karhunen–Loève Galerkin procedure, the governing equation of a given heat transfer problem is reduced faithfully to a model with a small degree of freedom. In our previous paper [4] it has been demonstrated that the dynamics of a flow reactor, governed by a convection-diffusion equation with a complicated flow field, can be described faithfully by a small number of ordinary differential equations with the help of the Karhunen–Loève Galerkin procedure. Therefore the number of equations to be solved in the inverse heat transfer problem is minimized when the Karhunen–Loève Galerkin procedure is employed, consequently reducing computational time greatly.

We apply this technique of inverse heat transfer employing the Karhunen–Loève Galerkin procedure to the estimation of time-varying strength of a heat source in a two-dimensional heat conduction system as depicted in Fig. 1. The system under consideration is a two-dimensional square domain with a time-varying heat source $G(t)$ located at $(x^{\dagger}, y^{\dagger})$. The thermal conductivity is assumed to be strongly dependent on temperature, making the governing equation nonlinear. The inverse problem at hand is the estimation of the unknown function $G(t)$ based on the temperature readings of a thermocouple located inside the domain.

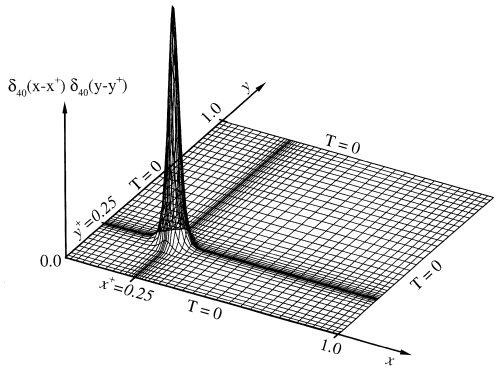


Fig. 1. The system and the shape and location of the function $\delta_{40}(x-x^{\dagger})\delta_{40}(y-y^{\dagger})$.

## 2. Theory

In this section, we explain briefly the Karhunen–Loève Galerkin procedure and the way how it is applied to the estimation of unknown strength of heat source in the domain. The original partial differential equation is eventually reduced to a set of ordinary differential equations by means of the Karhunen–Loève Galerkin procedure. The estimation of the strength of heat source in the domain is performed by using the conjugate gradient method.

### 2.1. The Karhunen–Loève decomposition

To make this paper self-contained, we introduce the essence of the Karhunen–Loève decomposition. The Karhunen–Loève decomposition, expressed briefly, is a method of representing a stochastic field with a minimum number of degree of freedom. As a means of explaining the Karhunen–Loève decomposition we select $N$ arbitrary irregularly shaped functions with $n = 1, 2, \ldots, N$. From now on, we call the irregular shapes of these functions $\{v_n\}$ 'snapshots'. In Park and Cho [4], it is shown that the most typical or characteristic structure $\phi(\boldsymbol{x})$ among these snapshots $\{v_n\}$ is given by solving the following eigenvalue problem of the integral equation (1):

$$\int_{\Omega} K(\boldsymbol{x}, \boldsymbol{x}')\phi(\boldsymbol{x}')\,\mathrm{d}\boldsymbol{x}' = \lambda\phi(\boldsymbol{x}) \tag{1}$$

where the kernel of the integral equation $K(\boldsymbol{x}, \boldsymbol{x}')$ is defined as,

$$K(\boldsymbol{x}, \boldsymbol{x}') = \frac{1}{N}\sum_{n=1}^{N} v_n(\boldsymbol{x})v_n^T(\boldsymbol{x}'). \tag{2}$$

Usually this kind of integral equation can be solved by means of the Schmidt–Hilbert technique [5].

Let's express the eigenvalues, $\lambda_1 > \lambda_2 > \cdots > \lambda_N$ and the corresponding eigenfunctions $\phi_1, \phi_2, \ldots, \phi_N$ in the order of magnitude of eigenvalues. The eigenfunction $\phi_1$ corresponding to the largest eigenvalue $\lambda_1$ is the most typical structure of the members of the snapshots $\{v_n\}$ and the eigenfunction $\phi_2$ with the next largest eigenvalue $\lambda_2$ is the next typical structure, and so forth. Since the kernel $K(\boldsymbol{x}, \boldsymbol{x}')$ is symmetric, these empirical eigenfunctions $\{\phi_n\}$ are mutually orthogonal. These empirical eigenfunctions $\{\phi_n\}$ can represent the system in the most efficient way. The Karhunen–Loève Galerkin procedure, employing these empirical eigenfunctions as trial functions of a Galerkin method, reduces the original system to a low dimensional model with a minimum degree of freedom.

### 2.2. The system and governing equations

The dimensionless governing equation for the unsteady heat conduction with a time-varying heat source with temperature dependent thermal conductivity in a two-dimensional square domain is given by

$$\frac{\partial T}{\partial t} = \frac{\partial}{\partial x}\left(\kappa \frac{\partial T}{\partial x}\right) + \frac{\partial}{\partial y}\left(\kappa \frac{\partial T}{\partial y}\right) + G(t)\delta_n(x - x^{\dagger})\delta_n(y - y^{\dagger}) \tag{3}$$

where all the variables are dimensionless, and $(x^{\dagger}, y^{\dagger})$ is the location of heat source. The relevant initial and boundary conditions are

$$T(x, y, t = 0) = 0 \tag{4a}$$

$$T(x = 0, y, t) = 0 \tag{4b}$$

$$T(x = 1, y, t) = 0 \tag{4c}$$

$$T(x, y = 0, t) = 0 \tag{4d}$$

$$T(x, y = 1, t) = 0. \tag{4e}$$

The function $\delta_n(x)$, which approximate the point source in the domain, is defined by:

$$\delta_n(x - x^{\dagger}) = \frac{n}{2\cosh^2(n(x - x^{\dagger}))} \tag{5}$$

and becomes the Dirac delta function as $n$ approaches infinity. In the present work, we take $n = 40$ with $(x^{\dagger}, y^{\dagger}) = (0.25, 0.25)$. The shape and strength of the point source $\delta_{40}(-x^{\dagger})\delta_{40}(y - y^{\dagger})$ is plotted in Fig. 1, together with the variable grid system $(40 \times 40)$ employed in the numerical computation. The dimensionless thermal conductivity $\kappa$ is assumed to depend on dimensionless temperature as follows:

$$\kappa = 1 + \alpha T \tag{6}$$

where $\alpha = 0.01$.

The governing equation (3) with the relevant boundary conditions is solved by a finite difference method with variable grids $(40 \times 40)$, which is found to be sufficient for the resolution of the temperature field. The inverse heat transfer problem under consideration is to estimate the unknown function $G(t)$ from the temperature recordings of a thermocouple positioned inside the domain.

### 2.3. Construction of empirical eigenfunctions

Before applying the Karhunen–Loève Galerkin procedure to reduce the degree of freedom of the system, we need a set of empirical eigenfunctions which capture the system behavior satisfactorily at least for the ranges of parameters of interest. These useful eigenfunctions can be obtained only from an ensemble of snapshots which are representative of the system characteristics. The low-dimensional model to be used in the inverse analysis should predict accurately the temperature distribution in the domain for a given heat source strength $G(t)$ located at $(x^{\dagger}, y^{\dagger})$. A set of temperature fields is obtained by solving equations (3)–(4) while imposing a step change on $G(t)$ from 0.0–25.0 and recording the transient temperature field at a certain time interval until the steady state is reached. We obtain 600 temperature fields in this way, which may be called the snapshots. When the Karhunen–Loève decomposition is applied to this ensemble of snapshots of the temperature field, we obtain a total of 600 empirical eigenfunctions in the order of their importance in characterizing the system. Figure 2 depicts typical snapshots and Fig. 3 shows the first, the second, the third, the eighth, the ninth and the tenth eigenfunctions with the corresponding normalized eigenvalues $\lambda_1 = 0.9675$, $\lambda_2 = 2.934 \times 10^{-2}$, $\lambda_3 = 2.830 \times 10^{-3}$, $\lambda_8 = 1.383 \times 10^{-7}$, $\lambda_9 = 2.451 \times 10^{-8}$ and $\lambda_{10} = 4.393 \times 10^{-9}$. Among the six eigenfunctions shown in Fig. 3, the empirical eigenfunctions with large eigenvalues (cf. Fig. 3a–c) represent the large scale structures of the temperature field, while empirical eigenfunctions with small eigenvalues (cf. Fig. 3d–f) represent the small scale structures of the temperature field.

### 2.4. The low-dimensional model

The Karhunen–Loève Galerkin procedure, which is a Galerkin method employing the above empirical eigenfunctions as basis functions, lumps the governing equation of the temperature field, equations (3)–(4), into a set of nonlinear ordinary differential equations. Assuming the temperature field $T(x, y, t)$ as a linear combination of empirical eigenfunctions as follows:

$$T(x, y, t) = \sum_{i=1}^{ME} a_i(t)\phi_i(x, y) \tag{7}$$

where $\phi_i$ is the $i$-th empirical eigenfunction, $a_i$ is the corresponding spectral coefficient and $ME$ is the total number of empirical eigenfunctions employed in the Kar-

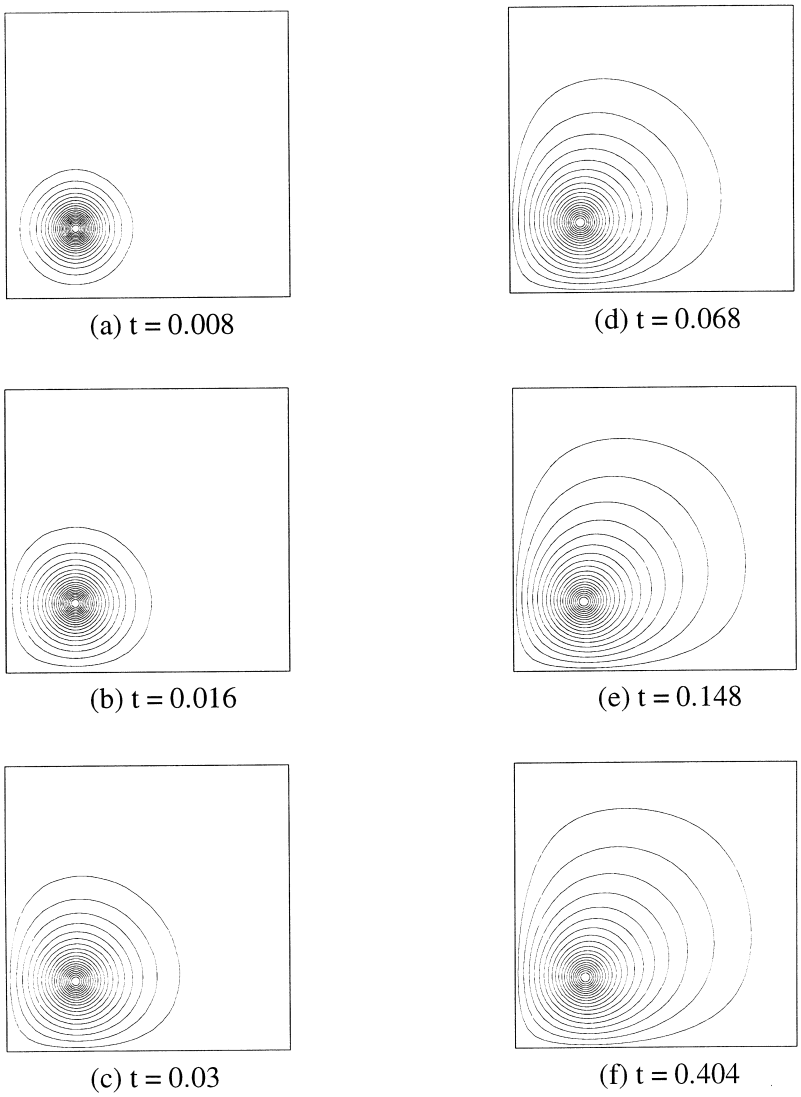


Fig. 2. Snapshots obtained at (a) $t = 0.008$, (b) $t = 0.016$, (c) $t = 0.03$, (d) $t = 0.068$, (e) $t = 0.148$, (f) $t = 0.404$.

hunen–Loève Galerkin procedure. The residual may be expressed as:

$$R \equiv \frac{\partial T}{\partial t} - \frac{\partial}{\partial x}\left(\kappa \frac{\partial T}{\partial x}\right) - \frac{\partial}{\partial y}\left(\kappa \frac{\partial T}{\partial y}\right) - G(t)\delta_n(x-x^{\dagger})\delta_n(y-y^{\dagger}). \quad (8)$$

Applying the Galerkin principle which enforces the residual to be orthogonal to each of the basis functions,

$$\int_{\Omega} R\phi_i \, \mathrm{d}\Omega = 0 \quad (i = 1, 2, \ldots, ME) \quad (9)$$

the equations (3)–(4) are reduced to the following set of nonlinear ordinary differential equations.

$$\frac{\mathrm{d}a_i}{\mathrm{d}t} + \sum_{j=1}^{ME} H_{ij}a_j + \alpha \sum_{j=1}^{ME}\sum_{l=1}^{ME} Q_{ijl}a_j a_l = G(t)S_i \quad (i = 1, 2, \ldots, ME) \quad (10)$$

where

$$H_{ij} = \int_{\Omega}\left(\frac{\partial \phi_i}{\partial x}\frac{\partial \phi_j}{\partial x} + \frac{\partial \phi_i}{\partial y}\frac{\partial \phi_j}{\partial y}\right)\mathrm{d}\Omega \quad (11)$$

$$Q_{ijl} = \int_{\Omega}\left(\frac{\partial \phi_i}{\partial x}\frac{\partial \phi_j}{\partial x} + \frac{\partial \phi_i}{\partial y}\frac{\partial \phi_j}{\partial y}\right)\phi_l \, \mathrm{d}\Omega \quad (12)$$

$$S_i = \int_{\Omega} \phi_i \delta_{40}(x-x^{\dagger})\delta_{40}(y-y^{\dagger}) \, \mathrm{d}\Omega. \quad (13)$$

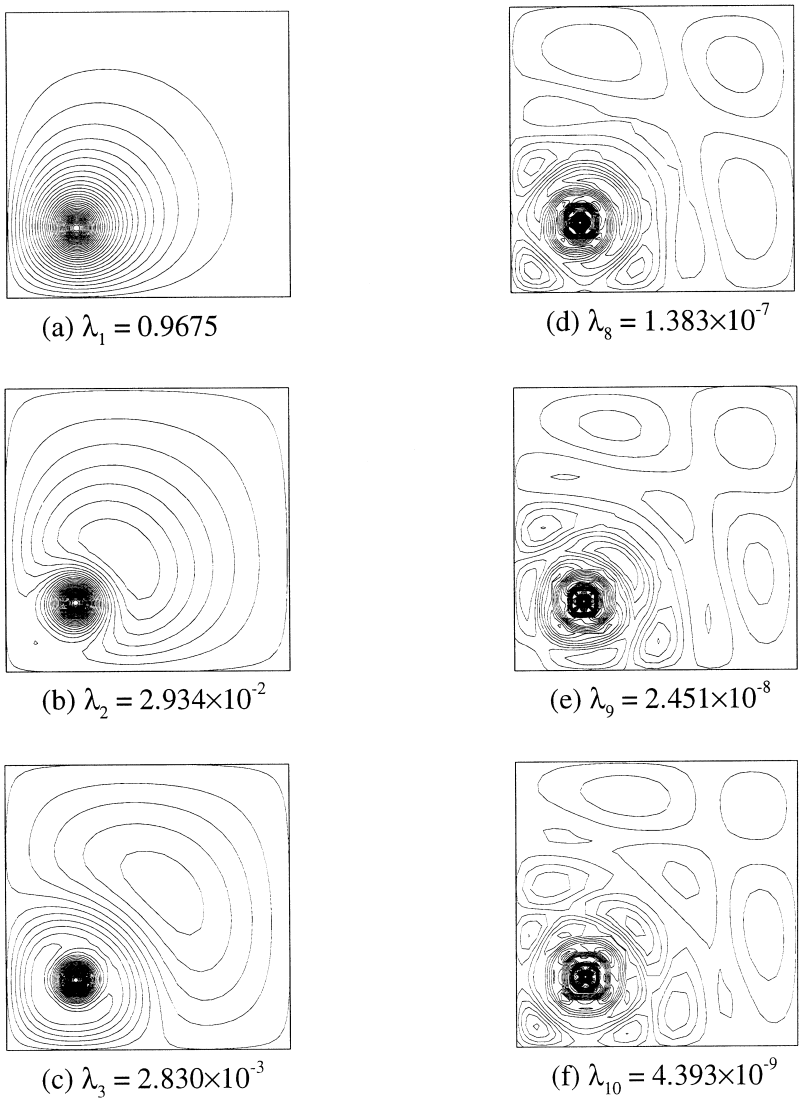


Fig. 3a–f. Some typical empirical eigenfunctions with the corresponding normalized eigenvalues.

Equation (10) can be easily solved by means of any ordinary differential equation solver.

The performance of the low-dimensional model equation (10) may be evaluated by comparing its solution with the finite difference solution of equation (3), which is regarded as the exact solution, for a given strength of heat source, $G(t)$. Usually the error of the low-dimensional dynamic model decreases as the number of eigenfunctions employed increases up to the optimal number of empirical eigenfunctions. But further increase of number of eigenfunctions beyond the optimal number does not improve the accuracy because the eigenfunctions with very small eigenvalues are contaminated with round-off errors. For the present work, the optimal number of empirical eigenfunctions is found to be 10, and thus we are going to employ 10 eigenfunctions for the construction of the low-dimensional dynamic model. The relative error of the low-dimensional model, constructed with 10 empirical eigenfunctions, is found to be less than 0.2% for the case of a step change of $G(t)$.

### *2.5. Solution of inverse problem employing the original nonlinear partial differential equation*

Before presenting the algorithm for solving the inverse problem employing the low dimensional dynamic model,

we first describe how to solve the same problem by the finite difference solution of the original nonlinear partial differential equation. The temperature field inside the domain, which can be easily measured at various locations, is determined by the heat source function $G(t)$. Therefore, $G(t)$ can be estimated by using the measured values of the temperature field at certain locations. The performance function for the identification of $G(t)$ is expressed by the sum of square residuals between calculated and observed temperature as follows:

$$J = \frac{1}{2}\sum_{m=1}^{MO}\int_0^{t_f}[T(x_m, y_m, t) - T^*(x_m, y_m, t)]^2\,dt \tag{14}$$

where $T(x_m, y_m, t)$ is the calculated temperature, $T^*(x_m, y_m, t)$ is the observed temperature at the location $(x_m, y_m)$, and $MO$ is the total number of measuring points. Although only one measuring point is employed in the present work (i.e., $MO = 1$), the summation over measuring points is kept to make the formula more general.

To minimize the performance function (14), we need the gradient of $J$, $\nabla J$, which is defined by

$$\delta J(G) \equiv J(G+\delta G) - J(G) = \int_0^{t_f} \nabla J \delta G\,dt \tag{15}$$

where $t_f$, the final time, is 0.2. The function $\nabla J$ can be obtained by introducing an adjoint variable $P(x, y, t)$, and rewriting the performance function as follows:

$$\begin{aligned} J(G) = {} & \frac{1}{2}\sum_{m=1}^{MO}\int_0^{t_f}[T(x_m, y_m, t) - T^*(x_m, y_m, t)]^2\,dt \\ & - \int_0^{t_f}\int_x\int_y P(x, y, t)\left[\frac{\partial T}{\partial t} - \frac{\partial}{\partial x}\left(\kappa\frac{\partial T}{\partial x}\right) - \frac{\partial}{\partial y}\left(\kappa\frac{\partial T}{\partial y}\right)\right. \\ & \left. - G(t)\delta_{40}(x - x^\dagger)\delta_{40}(t - y^\dagger)\right]dy\,dx\,dt. \end{aligned} \tag{16}$$

The variation of $J$, $\delta J$, is then given by the following equation:

$$\begin{aligned} \delta J(G) = {} & \sum_{m=1}^{MO}\int_0^{t_f}[T(x_m, y_m, t) \\ & - T^*(x_m, y_m, t)]\delta T(x_m, y_m, t)\,dt \\ & - \int_0^{t_f}\int_x\int_y P\left[\frac{\partial}{\partial t}\delta T\right. \\ & - \frac{\partial}{\partial x}\left(\kappa\frac{\partial}{\partial x}\delta T\right) - \frac{\partial}{\partial y}\left(\kappa\frac{\partial}{\partial y}\delta T\right) \\ & - \frac{\partial}{\partial x}\left(\delta\kappa\frac{\partial}{\partial x}T\right) - \frac{\partial}{\partial y}\left(\delta\kappa\frac{\partial}{\partial y}T\right) \\ & \left. - \delta G\delta_{40}(x - x^\dagger)\delta_{40}(y - y^\dagger)\right]dy\,dx\,dt. \end{aligned} \tag{17}$$

Integrating $\delta J$ by parts both in space and time, and exploiting the initial and boundary conditions for $T$ and $\delta T$, the gradient of $J$, $\nabla J$, in equation (15) is found to be as follows:

$$\nabla J = \int_x\int_y P(x, y, t)\delta_{40}(x - x^\dagger)\delta_{40}(y - y^\dagger)\,dy\,dx \tag{18}$$

while the adjoint variable $P(x, y, t)$ must satisfy:

$$\begin{aligned} \frac{\partial P}{\partial t} = {} & -\left(\frac{\partial}{\partial x}\kappa\frac{\partial P}{\partial x} + \frac{\partial}{\partial y}\kappa\frac{\partial P}{\partial y}\right) + \alpha\left(\frac{\partial P}{\partial x}\frac{\partial T}{\partial x} + \frac{\partial P}{\partial y}\frac{\partial T}{\partial y}\right) \\ & - \sum_{m=1}^{MO}[T(x, y, t) - T^*(x, y, t)]\delta(x - x_m)\delta(y - y_m) \end{aligned} \tag{19}$$

with the starting condition,

$$P(x, y, t = t_f) = 0 \tag{20}$$

and boundary conditions:

$$P(x = 0, y, t) = 0 \tag{21a}$$

$$P(x = 1, y, t) = 0 \tag{21b}$$

$$P(x, y = 0, t) = 0 \tag{21c}$$

$$P(x, y = 1, t) = 0. \tag{21d}$$

The function $\delta$ in equation (19) is the usual Dirac delta function. The Fletcher–Reeves method [6], which is one of the conjugate gradient methods, is successfully applied to the minimization of the performance function, using the gradient of $J$ determined by equation (18). The search direction or the conjugate direction at the first step is determined by:

$$d^0(t) = \nabla J(t) = \int_x\int_y P(x, y, t)\delta_{40}(x - x^\dagger)\delta_{40}(y - y^\dagger)\,dy\,dx. \tag{22}$$

Beginning the second iteration step, the conjugate direction is given by

$$d^n(t) = \nabla J^n(t) + \gamma^n d^{n-1}(t) \tag{23}$$

where

$$\gamma^n = \frac{\int_0^T (\nabla J^n(t))^2\,dt}{\int_0^T (\nabla J^{n-1}(t))^2\,dt} \tag{24}$$

and $n$ is the iteration number.

The optimal step length $\rho$ in the direction of $d^n$ is obtained by minimizing $J(G^n - \rho d^n)$ with respect to $\rho$. Formally, $J(G^n - \rho d^n)$ is expressed as:

$$\begin{aligned} J(G^n - \rho d^n) = {} & \frac{1}{2}\int_0^{t_f}\int_\Omega \sum_{m=1}^{MO}[T(x, y, t; G^n - \rho d^n) \\ & - T^*(x, y, t)]^2\delta(x - x_m)\delta(y - y_m)\,d\Omega\,dt. \end{aligned} \tag{25}$$

The directional derivative of $T$ at $G(t)$ in the direction of $d(t)$, denoted as $\delta T$, is defined by

$$\delta T = \lim_{\varepsilon \to 0} \frac{T(G+\varepsilon d) - T(G)}{\varepsilon}. \tag{26}$$

Then, the term $T(x, y, t; G^n - \rho d^n)$ in equation (25) is approximated by

$$T(x, y, t; G^n - \rho d^n) = T - (\delta T)\rho. \tag{27}$$

Substituting equation (27) into equation (25) and partially differentiating it with respect to $\rho$ and setting the resulting equation equal to zero, the value $\rho$ that minimizes $J(G^n - \rho d^n)$ is obtained as,

$$\rho = \frac{\delta J^n}{K^n} \tag{28a}$$

where

$$K^n = \sum_{m=1}^{MO} \int_0^{t_f} [\delta T(x_m, y_m, t)]^2 \, dt \tag{28b}$$

and

$$\delta J^n = \sum_{m=1}^{MO} \int_0^{t_f} [T(x_m, y_m, t) - T^*(x_m, y_m, t)] \delta T(x_m, y_m, t) \, dt. \tag{28c}$$

The updated heat source function $G^{n+1}(t)$ is obtained as

$$G^{n+1}(t) = G^n(t) - \rho d^n(t). \tag{29}$$

The sensitivity equation which determines $\delta T$ is given as follows:

$$\frac{\partial}{\partial t}\delta T = \frac{\partial}{\partial x}\left(\kappa \frac{\partial}{\partial x}\delta T\right) + \frac{\partial}{\partial y}\left(\kappa \frac{\partial}{\partial y}\delta T\right) + \frac{\partial}{\partial x}\left(\delta\kappa \frac{\partial T}{\partial x}\right) + \frac{\partial}{\partial y}\left(\delta\kappa \frac{\partial T}{\partial y}\right) + d(t)\delta_{40}(x - x^\dagger)\delta_{40}(y - y^\dagger) \tag{30}$$

where

$$\delta\kappa = \alpha \delta T. \tag{31}$$

The relevant initial and boundary conditions are,

$$\delta T(x, y, t = 0) = 0 \tag{32a}$$

$$\delta T(x = 0, y, t) = 0 \tag{32b}$$

$$\delta T(x = 1, y, t) = 0 \tag{32c}$$

$$\delta T(x, y = 0, t) = 0 \tag{32d}$$

$$\delta T(x, y = 1, t) = 0. \tag{32e}$$

The present algorithm is summarized below:

(1) Assume the heat source function $G(t)$ and calculate the temperature field $T$ by means of equation (3).
(2) Solve the adjoint problem [equations (19)–(21)].
(3) $\nabla J$ is determined by equation (18).
(4) The conjugate direction $d^n(t)$ is given by equation (23) with $\gamma^n$ determined by equation (24).
(5) Solve the sensitivity equations (30)–(32).
(6) The step length in the conjugate direction $d^n(t)$ is determined by equations (28a–c).
(7) The updated heat source function is obtained by equation (29).
(8) Repeat the above procedure until convergence.

### 2.6. Modified conjugate gradient approach [3, 7]

The conjugate gradient method employing the adjoint variable, as described in the previous section, usually converges fast, but it has one serious defect as noticed by other investigators [3]. The difficulty with this algorithm is that the value of heat source function at the final time, $G(t_f)$, will always be equal to the initial guess $G^0(t_f)$. The reason for this is explained by equations (18), (20), (22), (23) and (24). The difficulty encountered at the final time $t_f$ can be alleviated by the following modified conjugate method [3, 7].

We seek a continuously differentiable function $G(t)$ such that

$$G(t) = \int_a^t \frac{dG(t')}{dt'} dt'. \tag{33}$$

From equations (15) and (18), the variation of the performance function $\delta J$ may be rewritten as:

$$\delta J = \int_0^{t_f} \delta G(t) \int_\Omega P(x, y, t)\delta_{40}(x - x^\dagger)\delta_{40}(y - y^\dagger) \, d\Omega \, dt. \tag{34}$$

If equation (34) is integrated by parts with respect to the time variable, we find that

$$\delta J = -\int_0^{t_f} \frac{d\delta G}{dt} \int_{t_f}^t \int_\Omega \times P(x, y, t')\delta_{40}(x - x^\dagger)\delta_{40}(y - y^\dagger) \, d\Omega \, dt'. \tag{35}$$

Therefore, the derivative of $J$ with respect to $dG/dt$ is given by the following expression.

$$\nabla J\left(\frac{dG}{dt}\right) = -\int_{t_f}^t \int_\Omega P(x, y, t')\delta_n(x - x^\dagger)\delta_n(y - y^\dagger) \, d\Omega \, dt'. \tag{36}$$

Then, we take the conjugate direction as follows [3, 7]:

$$d^n(t) = \int_0^t D^n(t') \, dt' \tag{37}$$

where

$$D^n = \nabla J\left(\frac{dG}{dt}\right)^n + \gamma^n D^{n-1}. \tag{38}$$

Since $d^n(t_f)$, obtained by equation (37), is nonzero, the modified conjugate gradient method yields reasonably accurate value of $G(t_f)$ contrary to the regular conjugate gradient method. On the other hand, from equation (37) it can be seen that $d^n(0) = 0$. Then, for the same reason with the regular conjugate gradient method, the modified conjugate gradient method will not improve the starting value $G(0)$. In the present work, this dilemma is overcome by combining the regular and modified conjugate gradi-

ent method sequentially. At the first stage, we employ the modified conjugate gradient method for a certain number of iterations until a reasonably good estimation of the end value $G(t_f)$ is attained. Afterwards, the regular conjugate gradient method is adopted using the estimation of the modified conjugate gradient method as the initial approximation until the converged profile is obtained.

### 2.7. Solution of inverse problem employing the low-dimensional dynamic model of the Karhunen–Loève Galerkin procedure

Employing the low dimensional model equation (10) obtained by means of the Karhunen–Loève Galerkin procedure, one can also estimate the unknown heat source function $G(t)$ based on measurement of the temperature field at certain locations. The degree of freedom of equation (10) is only 10, whereas the degree of freedom of the original partial differential equation, which is equivalent to the grid number in the finite difference approximation, is $40\times40$ ($\approx1600$). Therefore, the procedure of solving inverse problems employing the low-dimensional model is predestined to be much faster than that employing the original nonlinear partial differential equation.

The performance function (14) may be rewritten in terms of the empirical eigenfunctions $\phi_i$ and corresponding spectral coefficients $a_i$ as:

$$J=\frac{1}{2}\sum_{m=1}^{MO}\int_0^{t_f}\left[\sum_{i=1}^{ME}a_i(t)\phi_i(x_m,y_m)-T^*(x_m,y_m,t)\right]^2\mathrm{d}t. \tag{39}$$

Following the same procedure as that in Section 2.5, the performance function (39) may be rewritten with the introduction of adjoint variables $p_k(t)$, $k=1,2,\ldots,ME$.

$$J(G)=\frac{1}{2}\sum_{m=1}^{MO}\int_0^{t_f}\left[\sum_{i=1}^{ME}a_i(t)\phi_i(x_m,y_m)-T^*(x_m,y_m,t)\right]^2\mathrm{d}t$$
$$-\int_0^{t_f}\sum_{k=1}^{ME}p_k(t)\left[\frac{\mathrm{d}a_k}{\mathrm{d}t}+\sum_{i=1}^{ME}H_{ki}a_i+\alpha\sum_{i=1}^{ME}\sum_{l=1}^{ME}Q_{kil}a_ia_l-G(t)S_k\right]\mathrm{d}t. \tag{40}$$

Then the gradient of the performance function, $\nabla J$, is found after integrating $\delta J$ by parts in time and exploiting the initial conditions for $\delta a_i(t)$ as follows:

$$\nabla J=\sum_{k=1}^{ME}p_k(t)S_k. \tag{41}$$

The adjoint variables $p_k(t)$ $(k=1,2,\ldots,ME)$ must satisfy the following ordinary differential equations,

$$\frac{\mathrm{d}p_k}{\mathrm{d}t}-\sum_{i=1}^{ME}p_iH_{ik}-\alpha\sum_{i=1}^{ME}\sum_{l=1}^{ME}p_iQ_{ikl}a_l-\alpha\sum_{l=1}^{ME}\sum_{i=1}^{ME}p_lQ_{lik}a_i$$
$$+\sum_{m=1}^{ME}\left[\sum_{i=1}^{ME}a_i\phi_i(x_m,y_m)-T^*(x_m,y_m,t)\right]\phi_k(x_m,y_m)=0$$
$$(k=1,2,\ldots,ME) \tag{42a}$$

with the following starting conditions at $t=t_f$:

$$p_k(t=t_f)=0\quad(k=1,2,\ldots,ME). \tag{42b}$$

The gradient of the performance function, $\nabla J$, given by equation (41) is exploited in the conjugate gradient method of Fletcher and Reeves [6] to minimize the performance function (39). The sensitivity equation for this case is given by:

$$\frac{\partial}{\partial t}\delta a_i+\sum_{k=1}^{ME}H_{ik}\delta a_k+\alpha\sum_{k=1}^{ME}\sum_{l=1}^{ME}Q_{ikl}\delta a_ka_l$$
$$+\alpha\sum_{k=1}^{ME}\sum_{l=1}^{ME}Q_{ikl}a_ka_l=d(t)S_i\quad(i=1,2,\ldots,ME) \tag{43a}$$

with the initial conditions,

$$\delta a_i(t=0)=0\quad(i=1,2,\ldots,ME). \tag{43b}$$

Here, $\mathrm{d}(t)$ is the conjugate direction which is updated in each iteration by the following rule:

$$d^n(t)=\nabla J^n(t)+\gamma^nd^{n-1}(t) \tag{44}$$

where

$$\gamma^n=\frac{\int_0^{t_f}(\nabla J^n(t))^2\,\mathrm{d}t}{\int_0^{t_f}(\nabla J^{n-1}(t))^2\,\mathrm{d}t} \tag{45}$$

with $\gamma^0=0$, and $n$ is the iteration number. The value of $\rho$ that minimizes $J(G^n-\rho d^n)$ is obtained, as previously, by differentiating $J(G^n-\rho d^n)$ with respect to $\rho$ and setting the resulting equation equal to zero:

$$\rho=\frac{\sum_{m=1}^{MO}\int_0^{t_f}\left[\sum_{i=1}^{ME}a_i(t)\phi_i(x_m,y_m)-T^*(x_m,y_m)\right]\times\left[\sum_{i=1}^{ME}\delta a_i(t)\phi_i(x_m,y_m)\right]\mathrm{d}t}{\sum_{m=1}^{MO}\int_0^{t_f}\left[\sum_{i=1}^{ME}\delta a_i(t)\phi_i(x_m,y_m)\right]^2\mathrm{d}t}. \tag{46}$$

The Fletcher–Reeves algorithm is applied to the inverse problem employing the low-dimensional dynamic model follows the procedure below:

(1) Assume $G(t)$ and calculate $a_i(t)$ $(i=1,2,\ldots,ME)$ using equation (10).
(2) Solve the adjoint problem with appropriate terminal conditions [equations (42a)–(42b)].
(3) The gradient of the performance function, $\nabla J$, is given by equation (41).
(4) The conjugate direction at the $n$-th iteration is given by equation (44), where $\gamma^n$ is given by equation (45).

(5) Solve the sensitivity equation with the relevant initial conditions, i.e., equations (43a)–(43b).
(6) Determine $\rho$ that minimizes $J(G^n-\rho d^n)$ by equation (46).
(7) The heat source function $G(t)$ is updated by

$$G^{n+1}(t) = G^n(t)-\rho d^n(t). \tag{47}$$

(8) Repeat the above calculations until convergence.

The regular conjugate gradient method applied to the low-dimensional dynamic model, as described above, has the same difficulty as what it has for the nonlinear partial differential equation, i.e., the heat source function at the terminal time, $G(t_f)$, is not updated since $\nabla J$ is zero at $t = t_f$ [cf. equations (41), (42b), (44), (45) and (47)]. This difficulty has been overcome by applying the modified conjugate gradient method and securing reasonably accurate final value of $G(t)$ before applying the regular conjugate gradient method as we have done for the original nonlinear partial differential equation (cf. Section 2.6).

## 3. Results

The inverse heat transfer problem we consider in the present investigation is the prediction of time-varying strength of a heat source from the knowledge of temperature recordings taken inside the domain (cf. Fig. 1). We consider three different cases of heat source function $G(t)$, as depicted in Fig. 4(a–c), and compare the accuracy and efficiency of the present method of solving this inverse conduction problem employing the Karhunen–Loève Galerkin procedure with those of the conventional method employing the original nonlinear partial differential equation (3). For brevity, we call the method employing the original partial differential equation the FDM-CG, and the method employing the low-dimensional model the KLG-CG. In both methods, the minimization of the performance function has been done by means of the conjugate gradient method suggested by Fletcher and Reeves [6]. The initial approximation of $G(t)$ is taken to 0.0 (constant) for all the numerical experiments described below.

The equations of $G(t)$ for the three cases shown in Fig. 4 are as follows:

Case (a)

$$G(t) = \tfrac{20}{0.06}t+2.5, \quad 0.0 \leqslant t \leqslant 0.06$$
$$G(t) = -\tfrac{15}{0.06}t+37.5, \quad 0.06 \leqslant t \leqslant 0.12$$
$$G(t) = 7.5 \quad 0.12 \leqslant t \leqslant 0.2 \tag{48}$$

Case (b)

$$G(t) = 100t+2.5, \quad 0.0 \leqslant t \leqslant 0.2. \tag{49}$$

Case (c)

$$G(t) = 2.5, \quad 0.0 \leqslant t \leqslant 0.06$$
$$G(t) = 22.5, \quad 0.06 \leqslant t \leqslant 0.14$$

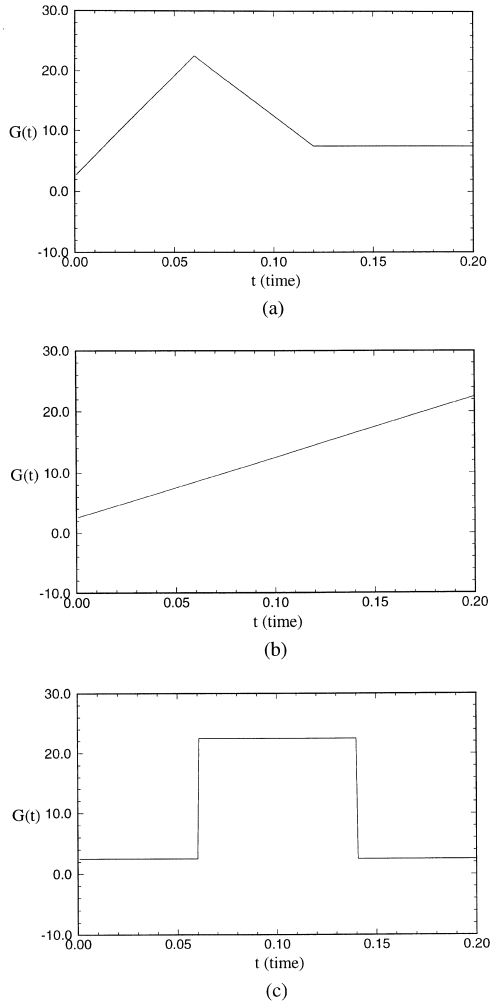


Fig. 4a–c. Various shapes of heat source functions considered in the present investigation.

$$G(t) = 2.5, \quad 0.14 \leqslant t \leqslant 0.2. \tag{50}$$

We quantify the accuracy of each method by defining the estimation error as follows:

$$\text{Error} = \frac{\|G_{\text{estimated}}-G_{\text{exact}}\|_{L2}^2}{\|G_{\text{exact}}\|_{L2}^2} \tag{51}$$

where $\|\cdot\|_{L2}$ is the usual $L_2$-norm. Equation (3) is solved by using a finite difference method and we adopt these numerical solutions as experimental measurements after adding small random noises. Namely,

$$T_{\text{measured}}(=T^*) = T_{\text{exact}}+\omega\sigma \tag{52}$$

where $\sigma$ determines the noise level, which takes values of 0.0, 0.05 or 0.08, and $\omega$ is a random number between $-2.576 < \omega < 2.576$. In fact, $\sigma$ is the standard deviation of measurement errors which are assumed to be the same

for all measurements, and $\omega$ is the Gaussian distributed random error. The above range of $\omega$ value corresponds to the 99% confidence bound for the temperature measurement.

To check the accuracy and efficiency of the new method of solving the inverse heat conduction problem, we first consider an idealized situation in which there are no measurement errors, i.e., $\sigma = 0.0$. The temperature recordings are assumed to be done continuously by a thermocouple located at the position $(0.4648, 0.2482)$ while the source is located at $(0.25, 0.25)$ as shown in Fig. 1. Figure 5(a–d) show the estimated heat source function $G(t)$ for the Case (a) when the regular conjugate gradient and the modified conjugate gradient method are employed in the FDM-CG and KLG-CG, respectively. The result of FDM-CG with regular conjugate gradient is plotted in Fig. 5(a), that of KLG-CG with regular conjugate gradient in Fig. 5(b), that of FDM-CG with modified conjugate gradient in Fig. 5(c), and finally that of KLG-CG with modified conjugate gradient in Fig. 5(d). As explained in Sections 2.5 and 2.6, it is shown that the regular conjugate gradient method does not improve the end point value $G(t_f)$ while the modified conjugate gradient method has the same problem with the starting point value $G(0)$ for both the FDM-CG and KLG-CG.

To overcome these difficulties, a combined iteration scheme, which combines the modified and regular conjugate gradient method sequentially, is employed to get the results presented in the following. Namely, at the first stage, we employ the modified conjugate gradient method for a certain number of iterations until a reasonably good estimation of the end point value $G(t_f)$ is attained. Afterwards, the regular conjugate gradient method is adopted using the estimation of the modified conjugate gradient method as the initial approximation to get the final converged profile. Figure 6 shows the convergence of the end point value $G(t_f)$ with respect to the iteration number for the Case (a) when using a modified conjugate gradient method. The error of $G(t_f)$ with the modified conjugate gradient method is defined by:

$$\text{Error} = \sum_{i=1}^{3} \frac{|G^n(t_f) - G^{n-1}(t_f)|}{|G^n(t_f)|} \tag{53}$$

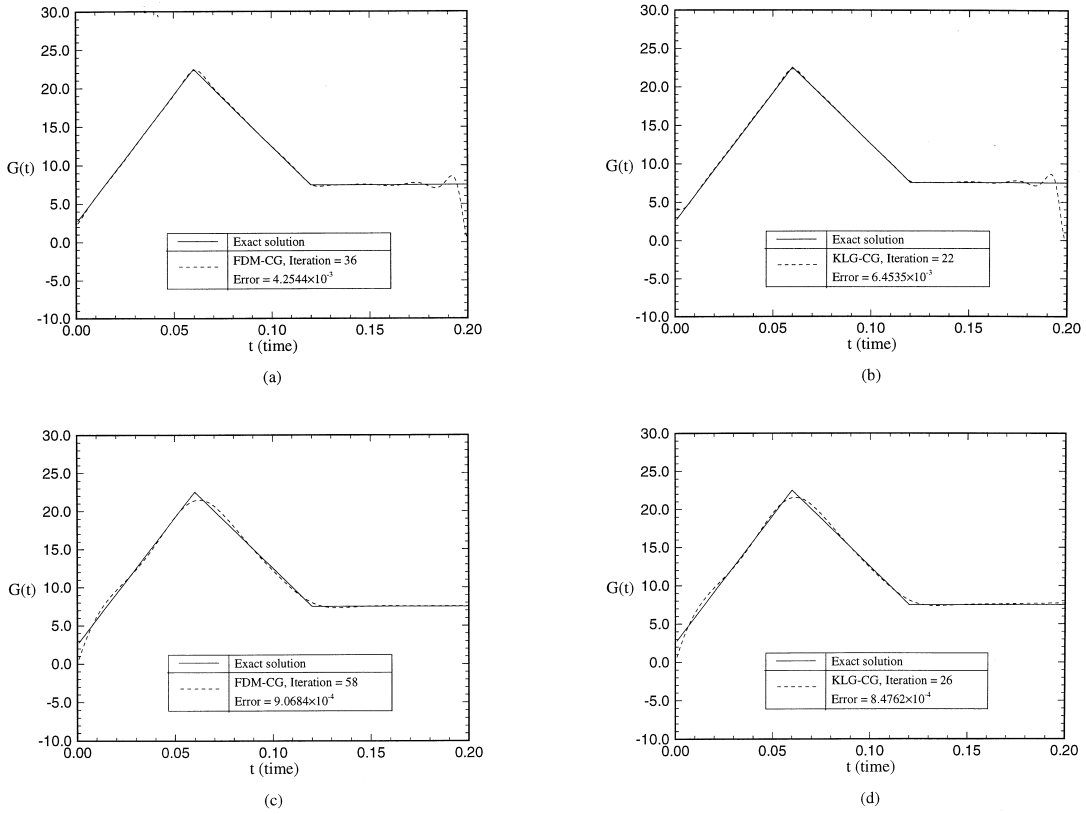


Fig. 5. The estimated profiles of heat source function. (a) FDM-CG employing the regular conjugate gradient method. (b) KLG-CG employing the regular conjugate gradient method. (c) FDM-CG employing the modified conjugate gradient method. (d) KLG-CG employing the modified conjugate gradient method.

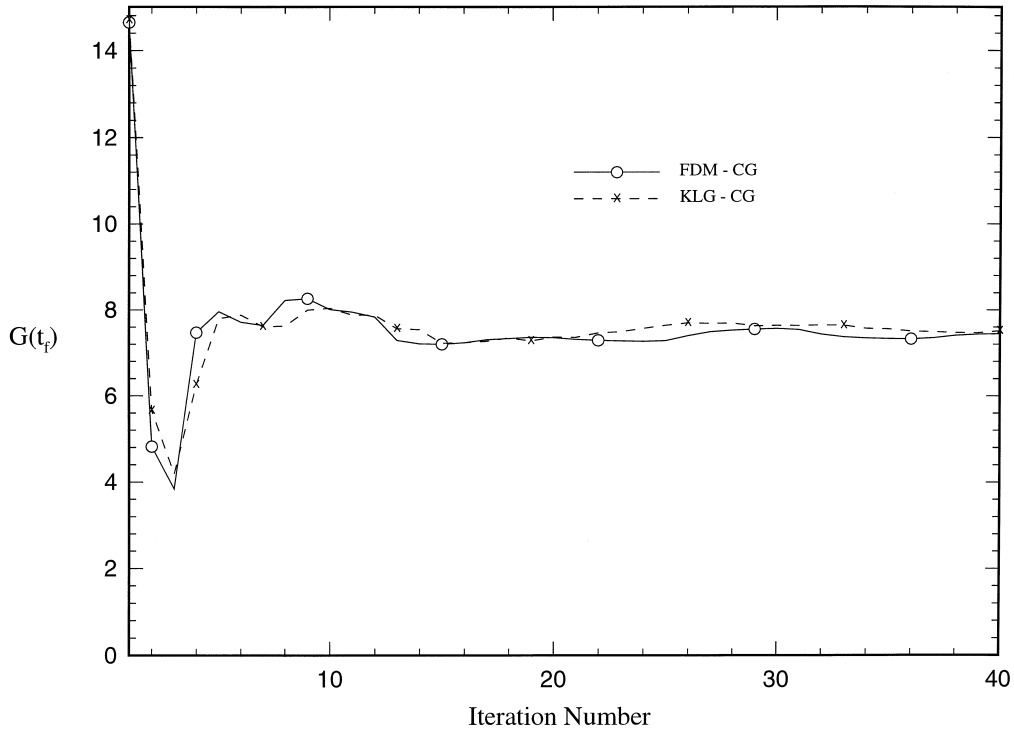


Fig. 6. The convergence of the end point value $G(t_f)$ with respect to iteration number when using the modified conjugate gradient method.

and the iteration of the modified conjugate gradient is stopped when $E_{mCG} < 0.01$.

Figure 7 depicts the convergence rate of the combined iteration scheme for the Case (a). The value of the performance function $J$ is reduced rapidly only after a couple of iterations both with the FDM-CG and KLG-CG. But we need usually many more iterations to make the starting point value $G(0)$ and the end point value $G(t_f)$ converged. Figures 8(a–b) show the estimated profile of heat source function for the Case (a). These results show that both the estimated profile based on the FDM-CG and that based on the KLG-CG are in excellent agreement with the exact heat source function over the whole domain, with the errors of the converged profiles, determined by equation (51), being $8.2494 \times 10^{-5}$ and $9.3383 \times 10^{-5}$, respectively. The numbers of iterations in the steps of modified conjugate gradient and regular conjugate gradient are also indicated in these figures. Similarly, the converged profiles of estimated heat source function for the Case (b) [equation (49)] are shown in Fig. 9(a) and (b) for the FDM-CG and the KLG-CG, with the estimation error of $2.6500 \times 10^{-4}$ and $2.6477 \times 10^{-4}$, respectively. Also shown in Fig. 10(a–b) are the converged profiles of $G(t)$ for the Case (c) [equation (50)], with the estimation errors of $9.0661 \times 10^{-3}$ (FDM-CG) and $9.5709 \times 10^{-3}$ (KLG-CG). For various shapes of the heat source function $G(t)$, one can obtain very accurate results by either FDM-CG or KLG-CG, when the noise level $\sigma$ is zero and the location of the thermocouple is at (0.4648, 0.2482).

Next, we consider the effects of noise level on the accuracy of the estimated profiles of heat source function when using the FDM-CG or the KLG-CG. In all practical experimental situations it is expected that some error will be induced into the measurements. When there are measurement errors, we have to use the following discrepancy principle for the stopping criterion of the iterative procedure of the conjugate gradient method [3, 8]. We assume

$$T(x_m, y_m) - T^*(x_m, y_m) \approx \sigma. \tag{54}$$

Introducing this result into equation (14), we find

$$J \approx \frac{1}{2} \int_0^{t_f} \sum_{m=1}^{MO} \sigma^2 \, dt \equiv \varepsilon^2. \tag{55}$$

Then the discrepancy principle for the stopping criterion is taken as

$$J < \varepsilon^2. \tag{56}$$

If the functional $J$ has a minimum value that is larger

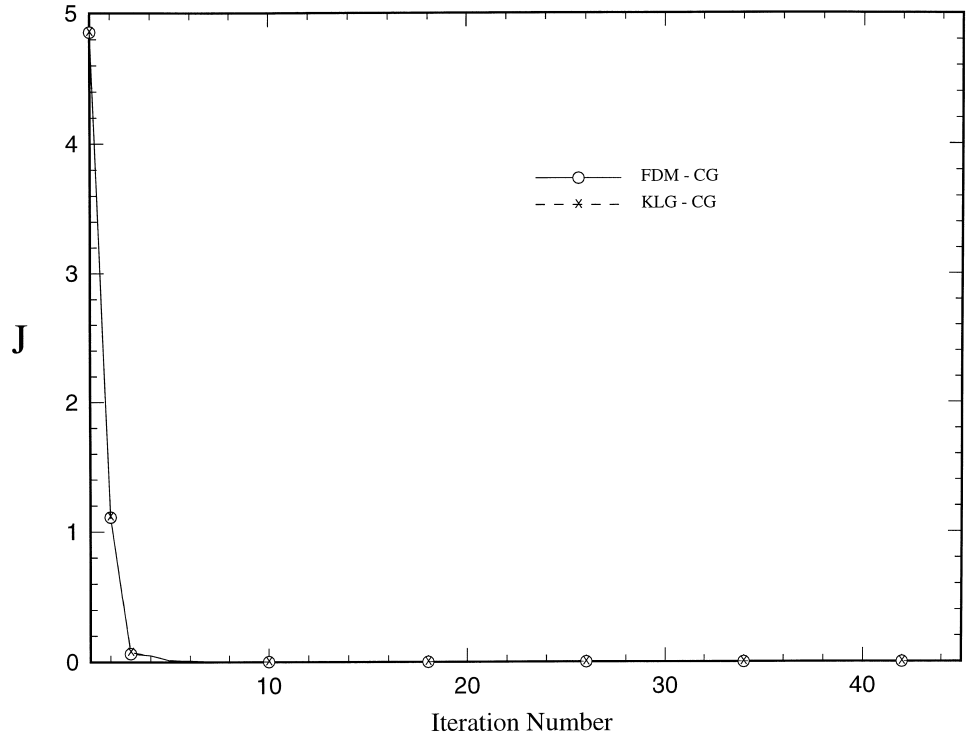


Fig. 7. Convergence rate of the combined iteration scheme. The value of the performance function $J$ is reduced rapidly only after a couple of iterations both with the FDM-CG and KLG-CG.

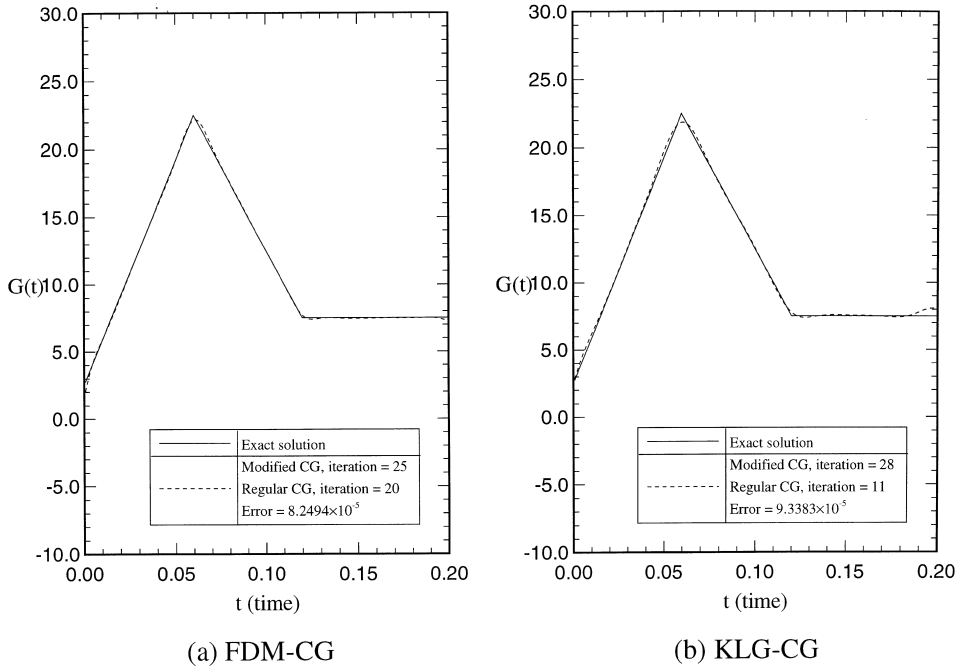


Fig. 8. The estimated profiles of heat source function for the Case (a) when the combined iteration scheme is employed. (a) FDM-CG, (b) KLG-CG.

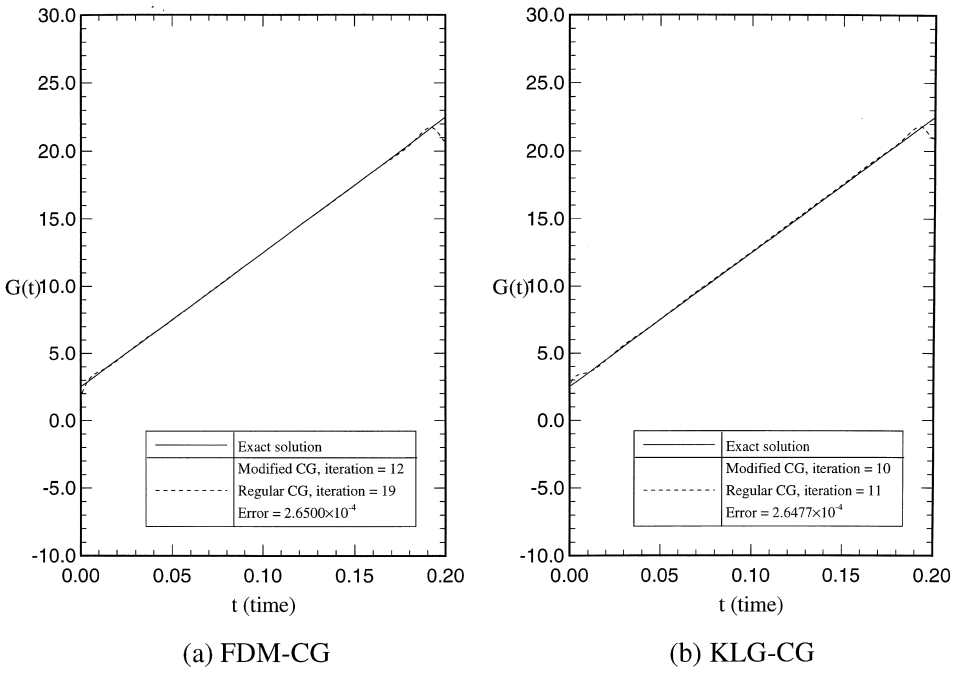


Fig. 9. The estimated profiles of heat source function for the Case (b). (a) FDM-CG, (b) KLG-CG.

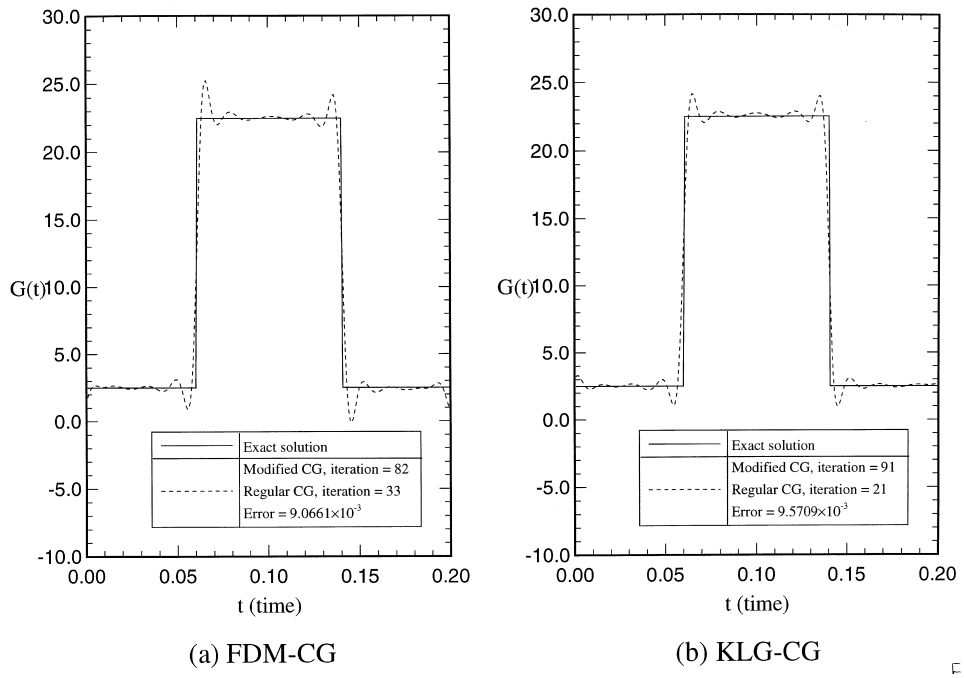


Fig. 10. The estimated profiles of heat source function for the Case (c). (a) FDM-CG, (b) KLG-CG.

than $\varepsilon^2$, the following criterion is used to stop the iteration:

$$J(G^{(i+1)}) - J(G^{(i)}) < \varepsilon_1 \tag{57}$$

where $\varepsilon_2$ is a prescribed small number.

Figures 11(a–d) show the estimated heat source functions obtained either by the FDM-CG or by the KLG-CG for various values of the noise level $\sigma$. If the noise level is the same ($\sigma = 0.05$ or $\sigma = 0.08$), the accuracy of the FDM-CG and the KLG-CG is almost the same. These figures also reveal that with both the FDM-CG and KLG-CG, the accuracy deteriorates as the noise level increases.

Figures 12(a–d) show the effect of location of thermocouple on the accuracy of the estimated heat source function. In addition to the previous default location $(x_m, y_m) = (0.4648, 0.2482)$, we consider two more locations farther from the heat source than the default one, i.e., $(0.6008, 0.2482)$ and $(0.7183, 0.2482)$. Figures 12(a–b) are for $(0.6008, 0.2482)$ and Figs 12(c–d) are for $(0.7183, 0.2482)$ when $\sigma = 0$. Comparing results of Figs 8(a–b) with those of Figs 12(a–d), we find that as the location of thermocouple approaches that of heat source, the accuracy improves both with the FDM-CG and the KLG-CG, since the sensitivity of the temperature field with respect to the heat source increases as the distance between the measurement point and the heat source decreases.

One of the most important results in the present investigation is the comparison of CPU time required when estimating the heat source function by employing either the FDM-CG or the KLG-CG. When the Ultrasparc workstation is used, it takes only 6 s for the KLG-CG to yield the converged profile of heat source function for the Case (a) [cf equation (48)], whereas it takes 15 min 21 s for the FDM-CG to generate the same result. If the computer codes adopted in the present investigation were optimized, the CPU time for both methods will be reduced proportionally. This drastic reduction in CPU time when employing the KLG-CG is easily expected from the fact that the degree of freedom of low-dimensional dynamic model is far less than that of the original nonlinear partial differential equation.

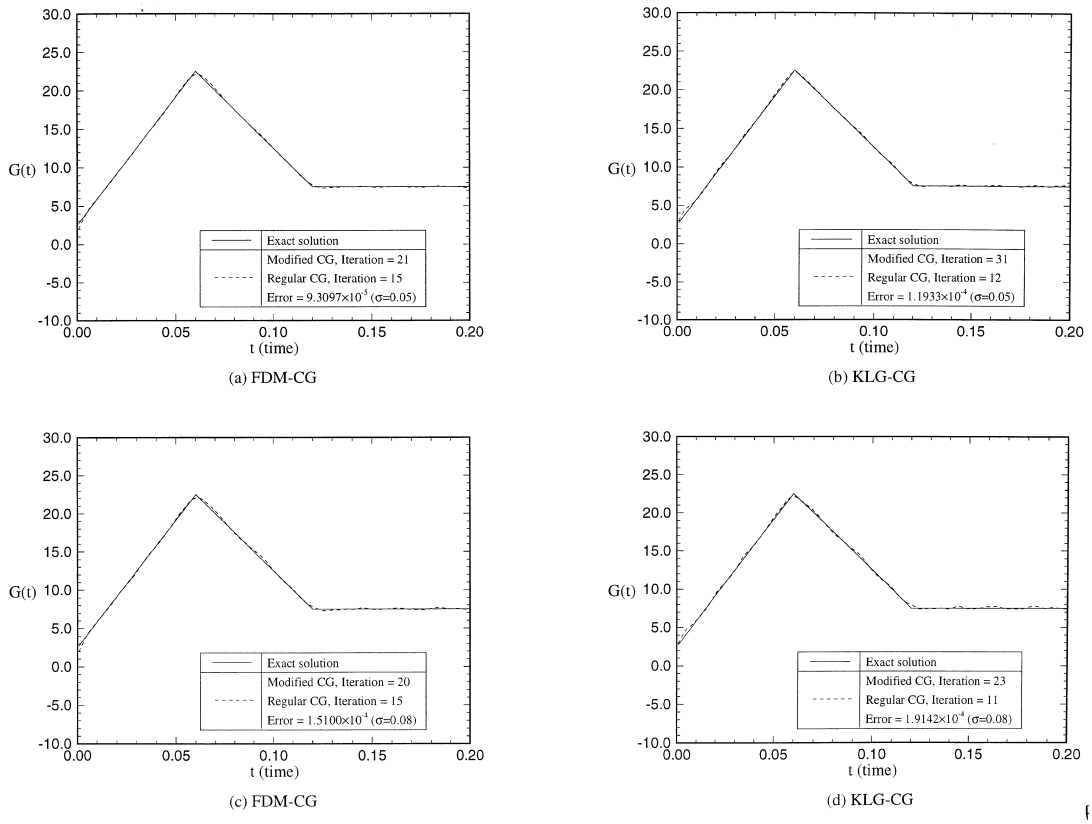


Fig. 11. The estimated profiles of heat source function for the Case (a), when the noise level $\sigma$ is not zero. (a) FDM-CG, $\sigma = 0.05$, (b) KLG-CG, $\sigma = 0.05$, (c) FDM-CG, $\sigma = 0.08$, (d) KLG-CG, $\sigma = 0.08$.

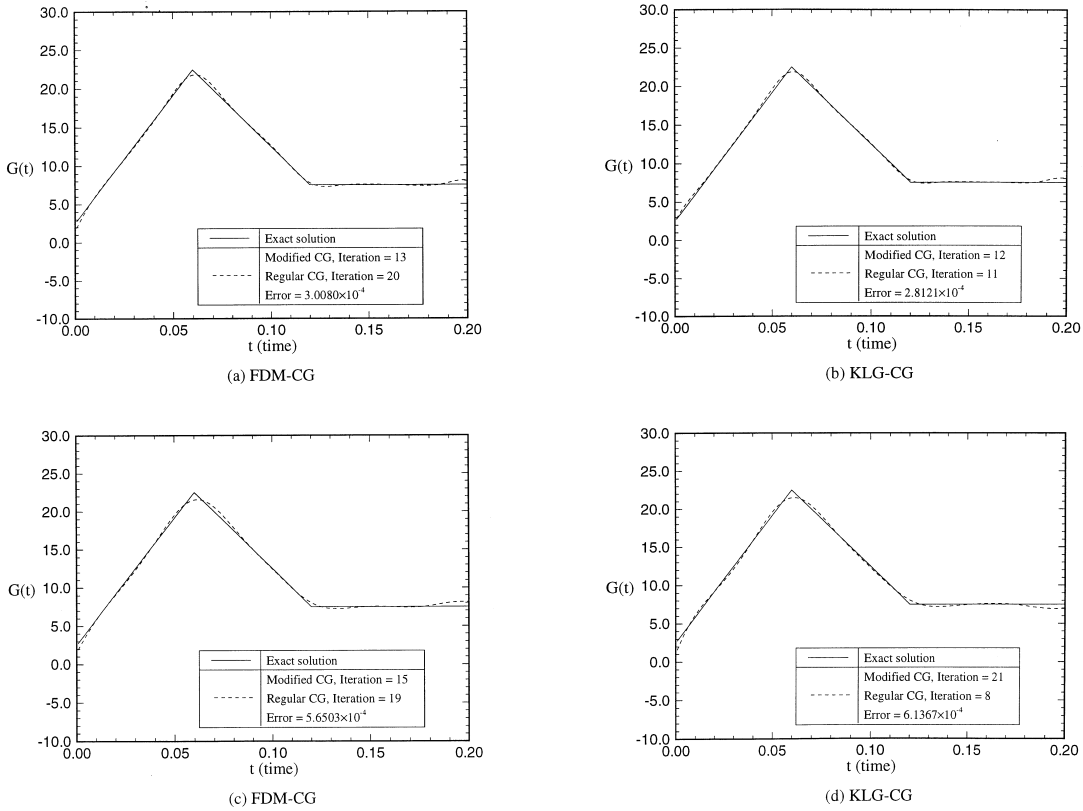


Fig. 12. The effect of location of thermocouple on the accuracy of the estimated heat source function. (a) FDM-CG, $(x_m, y_m) = (0.6008, 0.2482)$, (b) KLG-CG, $(x_m, y_m) = (0.6008, 0.2482)$, (c) FDM-CG, $(x_m, y_m) = (0.7183, 0.2482)$, (d) KLG-CG, $(x_m, y_m) = (0.7183, 0.2482)$.

## 4. Conclusions

The Karhunen–Loève Galerkin procedure is employed for the solution of the inverse problem of determining the time-varying strength of a heat source based on temperature recordings inside the domain. The performance function, which is the sum of square residuals between calculated and observed temperature, is minimized by using the conjugate gradient method. This method of solving inverse heat transfer problems, called KLG-CG in the present paper, has been compared with the traditional method employing the original partial differential equation (FDM-CG) in terms of accuracy and efficiency. The present investigation reveals that the KLG-CG yields estimations as accurate as the FDM-CG for various shapes of heat source function with various degree of noise levels. The degree of freedom of the low-dimensional model from the Karhunen–Loève Galerkin procedure is only 10, whereas that of the finite difference solution of the original partial differential equation is about 1600. This drastic reduction in degree of freedom with the use of the KLG-CG as compared to the FDM-CG reduces the computer time tremendously without deteriorating accuracy in the inverse analysis.

## References

[1] J.V. Beck, K.J. Arnold, Parameter Estimation in Engineering and Science, John Wiley and Sons, New York, 1977, p. 444.

[2] Y. Jarney, M.N. Özisik, J.P. Bardon, A general optimization method using adjoint equation for solving multidimensional inverse heat conduction, International Journal of Heat and Mass Transfer 34 (1991) 2911–2919.

[3] A.J. Silva Neto, M.N. Özisik, Two-dimensional inverse heat conduction problem of estimating the time-varying strength of a line heat source, Journal of Applied Physics 71 (11) (1992) 5357–5362.

[4] H.M. Park, C.H. Cho, Low dimensional modeling of flow reactors, International Journal of Heat and Mass Transfer 39 (16) (1996) 3311–3323.

[5] R. Courant, D. Hilbert, Methods of Mathematical Physics, vol. 1, Wiley-Interscience, New York, 1962, p. 115.
[6] R. Fletcher, R.M. Reeves, Function minimization by conjugate gradients, The Computer Journal 7 (1964) 149–154.
[7] O.M. Alifanov, V.V. Mikhailov, Solution of the nonlinear inverse thermal conductivity problem by the iteration method, J. Engng Phys. 35 (6) (1978) 1501–1506.
[8] O.M. Alifanov, Application of the regularization principle to the formulation of approximate solution of inverse heat conduction problem, J. Engng Phys. 23 (6) (1972) 1566–1571.